Integration of Dynamic Multiphase Flow and Reservoir Models for Improved Oil Recovery Simulation

Charith Rajapaksha, Ismail Hossain Rafi, Nirajan Raut, Ali Moradi, Soheila Taghavi, Britt M. E. Moldestad

Department of Process and Environmental Technology, University of South-Eastern Norway, Norway.
{charithpriya@gmail.com, ismailrafi16@gmail.com, nirajanraut8@gmail.com, ali.moradi@usn.no, soheila.t.hosnaroudi@usn.no , britt.moldestad@usn.no}

Abstract: The utilization of advanced multilateral wells to enhance well-reservoir contact, coupled with water injection, stands out as a common approach to boost oil extraction efficiency. It is imperative to develop precise, fully integrated, dynamic, well-reservoir models tailored for this type of oil recovery to enhance the design of advanced multilateral well completions. This study addresses the challenge by constructing a well model using OLGA®, which is, a dynamic multiphase flow simulator, and a reservoir model using Eclipse™, a reservoir simulator. Subsequently, these models are seamlessly integrated to perform comprehensive simulations. The proposed approach is tested on a case study involving oil recovery through an advanced multilateral well completed with various Flow Control Devices (FCDs) supported by water injection. Results from the simulations demonstrate the success of the integration approach, offering a reliable method for accurately modelling oil recovery from advanced multilateral wells to improve oil recovery. Notably, according to this study, wells completed with Autonomous Inflow Control Valves (AICVs) exhibit superior performance, optimizing oil recovery with a reduced carbon footprint.

Keywords: Advanced multilateral wells, Well-reservoir model, Autonomous Inflow Control Valve, Autonomous Inflow Control Devices, Inflow Control Devices.

1. INTRODUCTION

Even though the world is moving towards renewable energy, crude oil is still significantly contributing to the world's energy demand. Despite advances, a considerable portion of oil remains unrecovered due to traditional technologies.

The multilateral well model can be implemented to increase the oil recovery, a well-completion technique more suitable for horizontal drilling. This method has several advantages, such as increased reservoir exposure, reduced water and gas coning, accelerated production, connecting high permeability areas, and lower capital costs than constructing single-well systems, although with disadvantages like early water and gas breakthrough (Elyasi, 2016). Figure 1 illustrates the main types of multilateral wells used in industry.

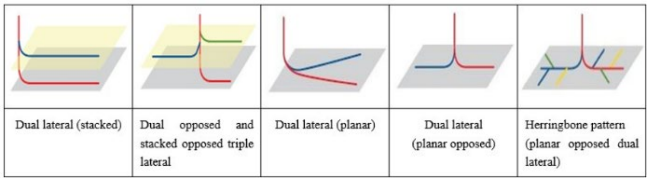

Fig. 1. Types of different multilateral wells (Flatern, 2021).

Methods like polymer and zonal control with flow control devices (FCDs) tackle early breakthroughs and increase oil recovery. Inflow control devices (ICDs), Autonomous Inflow Control Devices (AICDs), and Autonomous Inflow Control Valves (AICVs) are mainly used as FCDs in the industry, which makes the oil well an advanced well (Aakre *et al.*, 2014).

To design and maintain advanced multilateral wells, a proper simulation and modelling are to be done to decide the parameter values for optimum production. Oil recovery through advanced multilateral wells is a transient process, and the simulation model must capture the transient interaction between the reservoir and the well. Therefore, a dynamic, fully coupled, well-reservoir model is required to simulate oil recovery accurately through advanced wells. Researchers widely use the multisegmented well (MSW) model to simulate advanced wells, but it is a homogeneous model and is not very accurate due to simplifications. Coupling the well model in a dynamic multiphase simulator with a reservoir model can be used to overcome the inaccuracies. This study was conducted to study the coupling well model in the OLGA multiphase simulator with a reservoir model done in ECLIPSE.

2. MULTISEGMENT WELL MODEL

The multisegmented well model in ECLIPSE is an advanced extension for accurately modelling fluid behaviour in advanced wells. It divides the production tubing into multiple one-dimensional segments with independent variables to describe the conditions. These variables are determined by solving material balance equations for each phase and

component using different pressures. This approach allows for precisely modelling the relationship between pressure gradients and fluid composition changes in advanced wells (Anuththara *et al.*, 2023).

Figure 2 presents a schematic of an MSW model for an advanced horizontal well. This model treats the production tubing and wellbore as distinct branches of specific segments. Additionally, segments can be designed to simulate Flow Control Devices (FCDs). These FCDs connect the wellbore and production tubing, as depicted in Fig. 2. Fluids enter the wellbore through its segments, pass through FCD valve segments into the production tubing, and then flow to the production outlet via the production tubing segments (Anuththara *et al.*, 2023).

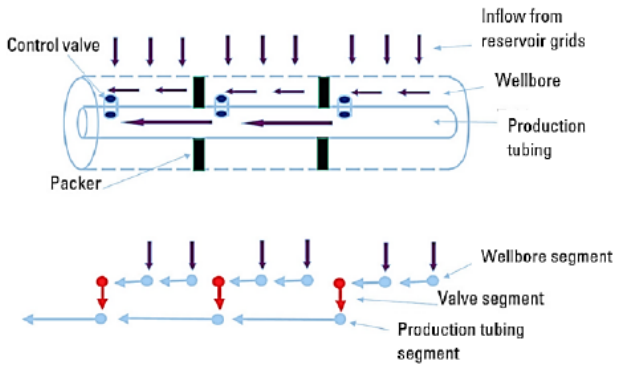

Fig. 2. Schematic of a multisegmented well model (Moradi *et al., 2022a).*

3. FLOW CONTROL TECHNOLOGY

Flow control devices (FCDs) are applied to prevent early gas and water breakthroughs in a well, making it an advanced well. The inflow control technology is essential for improving oil recovery and expanding reservoir lifespan, making oil production economical.

3.1 Inflow control device (ICD)

ICD is a passive inflow control device without any active part that can adjust the flow with the conditions. It limits the flow by giving an additional pressure drop to achieve a distributed flow profile along the horizontal well with the pre-determined design, as shown in Fig. 3,

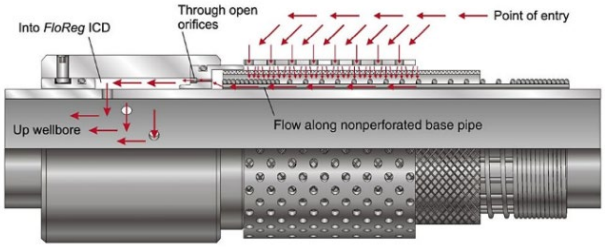

Fig. 3. Orifice-type ICD and its flow path (Mathiesen *et al.*, 2014).

Several ICDs are usually placed along the well tubing, and with an even production rate along the well, the water and gas breakthroughs can be delayed. However, ICDs cannot control the flow after the breakthrough and choke the low viscous fluids into the production tubing. The governing equation for orifice-type ICD is mentioned as follows (Moradi *et al.*, 2022b),

$$\dot{Q} = C_D A \sqrt{\frac{1}{1-\beta^4}} \sqrt{\frac{2\Delta P}{\rho}} \quad , \tag{1}$$

Where,
$\dot{Q}$ is the volume flow rate of the fluid through the ICD
ΔP is the pressure drop over the ICD
ρ is the fluid density
A is the cross-sectional area of the ICD nozzle
C_D is the discharge coefficient, which depends on the ICD design

3.2 Autonomous inflow control device (AICD)

AICD is an improved version of ICDs that can delay the water and gas breakthroughs and partially be close to low-viscosity fluids like water and gases. AICD has active and passive control elements to produce a pressure drop and control the flow autonomously.

Figure 4 presents a schematic of the rate control production (RCP) type AICD, which consists of a free-floating disc, an outer seat, and an inner seat (Anuththara *et al.*, 2023). According to the pressure, forces acting on the disc will move to control the flow accordingly.

When a low viscous fluid compared to oil flows through the valve, a low pressure will be created in the inlet area due to low friction force, according to Bernoulli's equation. This pressure reduction creates a force that pulls the moving plate toward the inlet, partially closing the valve. This mechanism enables these valves to autonomously reduce the flow rate of unwanted fluids such as water or gas (Moradi *et al.*, 2022b).

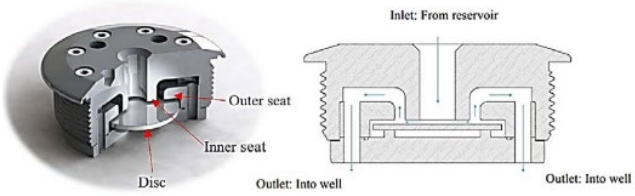

Fig. 4. Schematic diagram of Statoil's RCP valve (Anuththara *et al.*, 2023).

The empirical equation pressure drop across an RCP-type AICD is as follows,

$$\Delta P = a_{AICD} \cdot \left(\frac{\rho_{mix}{}^2}{\rho_{cal}}\right) \cdot \left(\frac{\mu_{cal}}{\mu_{mix}}\right)^y \cdot \dot{Q}^x \quad , \tag{2}$$

where,
$\dot{Q}$ is the volume flow rate of the fluid through the AICD
ΔP is the pressure drop over the AICD
ρ_{mix} is the density of the fluid mixture
μ_{mix} is the viscosity of the fluid mixture

a_{AICD}, x and y are user input parameters that depend on the AICD design and the fluid properties, while ρ_{cal} and μ_{cal} are calibrating parameters. ρ_{mix} and μ_{mix} are calculated as follows,

$$\rho_{mix} = \alpha_{oil}\rho_{oil} + \alpha_{water}\rho_{water} + \alpha_{gas}\rho_{gas} \quad , \tag{3}$$

$$\mu_{mix} = \alpha_{oil}\mu_{oil} + \alpha_{water}\mu_{water} + \alpha_{gas}\mu_{gas}\ , \quad (4)$$

where,
α_{oil} is the volume fraction of oil in the mixture
α_{water} is the volume fraction of water in the mixture
α_{gas} is the volume fraction of gas in the mixture

3.3 Autonomous inflow control valve (AICV)

AICV is the latest inflow control device developed by InflowControl AS, which has been claimed to have better choking performance than AICD and ICD. AICV can almost entirely close its opening to unwanted fluids with low viscosities, such as water and gas.

AICV consists of two restrictors where: one is a laminar restrictor, and the other is a turbulent restrictor. Figure 5 illustrates a schematic diagram of an AICV and how the pressure gradients stack where oil gets and lower pressure drops, allowing it to pass while the valve chokes water and gas (Moradi *et al.*, 2022b).

The pressure drops in the laminar and turbulent restrictors are calculated as follows,

$$\Delta P_{Laminar} = \frac{32\mu\rho v L}{D^2}\ , \quad (5)$$

$$\Delta P_{Turbulent} = \frac{k\rho v^2}{2}\ , \quad (6)$$

Where,
ΔP is the pressure drop over the restrictor
μ is the fluid viscosity
ρ is the fluid density
v is the fluid velocity
L is the laminar restrictor length
D is the laminar restrictor diameter
k is the geometrical constant

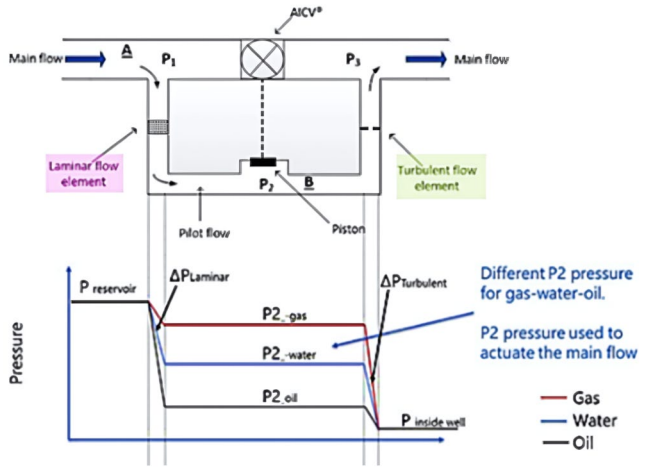

Fig. 5. A simplified sketch of the flow paths in AICV and pressure changes inside for different fluids (Anuththara et al. 2023).

Equation 5 explains how the pressure drops in the laminar restrictor depend on the fluid density and viscosity. Therefore, when low viscous fluid like water and gases pass through the restrictor, it gets a low-pressure drop compared to a high viscous fluid such as heavy oil. Because of this low-pressure drop, low viscous fluids have a higher pressure in the chamber between the restrictors, leading to higher velocity before passing through the turbulent restrictor. As Equation 6 mentions, low viscous fluids experience a higher pressure drop than oil across the turbulent restrictor, which allows the AICV to remain open for oil while it is almost closed for water and gas (Moradi *et al.*, 2022b).

The performance criteria for AICV and AICD mentioned in Fig. 6 were used in this study where AICV closes its opening 60% when the water cut reaches 1, while AICD can close nearly 20% of its opening. The plots in Fig. 6 were obtained based on the experimental results of AICD and AICV for a fluid with the properties discussed in Chapter 4.1.

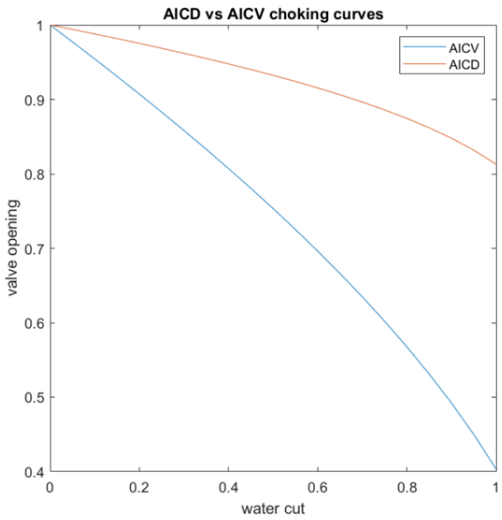

Fig. 6. Choking functionality comparison between AICV and AICD.

4. RESERVOIR MODEL IN ECLIPSE

4.1 Reservoir fluid and rock properties

The reservoir conditions and fluid properties used in this study were similar to the Troll field in the North sea which also used to obtain AICV/AICD test data. Table 1 presents the reservoir and fluid properties used for the simulations.(Anuththara *et al.*, 2023).

Table 1. Reservoir properties and rock properties

Parameter	Value
Oil density	890 kg/m^3
Water density	1000 kg/m^3
Gas density	0.67 kg/m^3
GOR	50 Sm^3/ Sm^3
Reservoir Pressure	130 bara
Water viscosity	0.45 cp
Oil viscosity	2.7 cp
Porosity	0.15 – 0.27
Temperature	68 ^{0}C

4.2 Reservoir grid

The dimensions of the reservoir are illustrated in Table 2. Figure 7 presents the 3D image of the reservoir is presented. The reservoir has two layers separated by a shale layer with a thickness of 50 m. From the 10th cell, the water is injected into the reservoir.

Table 2: Dimensions of the reservoir

Length of the reservoir (x)	1250 m
Width of the reservoir (y)	500 m
Height of the reservoir (z)	140 m

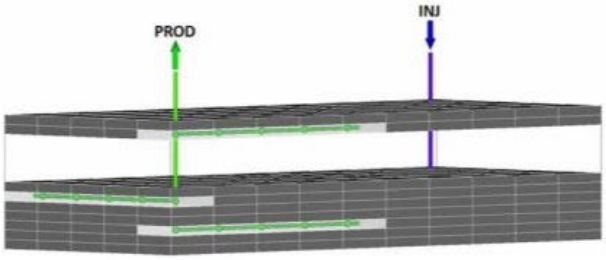

Fig. 7. Topology of the reservoir.

4.3 Reservoir permeability

The reservoir is considered a homogeneous reservoir with the same porosity and permeability. The long-normal absolute permeability is assumed in the 100-500 mD range.

Figure 8 represents the relative permeability curves for water (k_{rw}) and oil (k_{ro}) with the water saturation (S_w) used in this study, which was developed using Corey model.

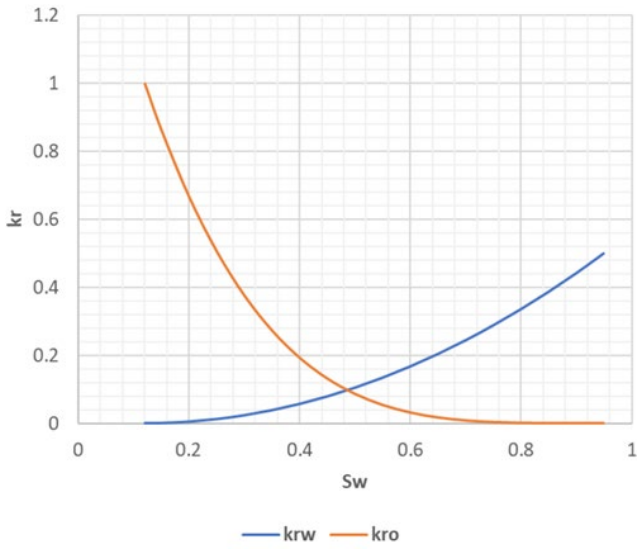

Fig. 8. Relative permeability curves.

4.4 Initial conditions

The reservoir developed with ECLIPSE has three different zones. Therefore, the pressure, oil, water, and gas saturation change along the depth.

Initially, the reservoir pressure is 130 bar at 68ºC, increasing as the depth rises. The depth of oil-water contact (OWC) and gas-oil contact (GOC) are 2300 m and 2010m, respectively. Therefore, the pressure increases as the depth increases per hydrostatic pressure, as shown in Fig. 9.

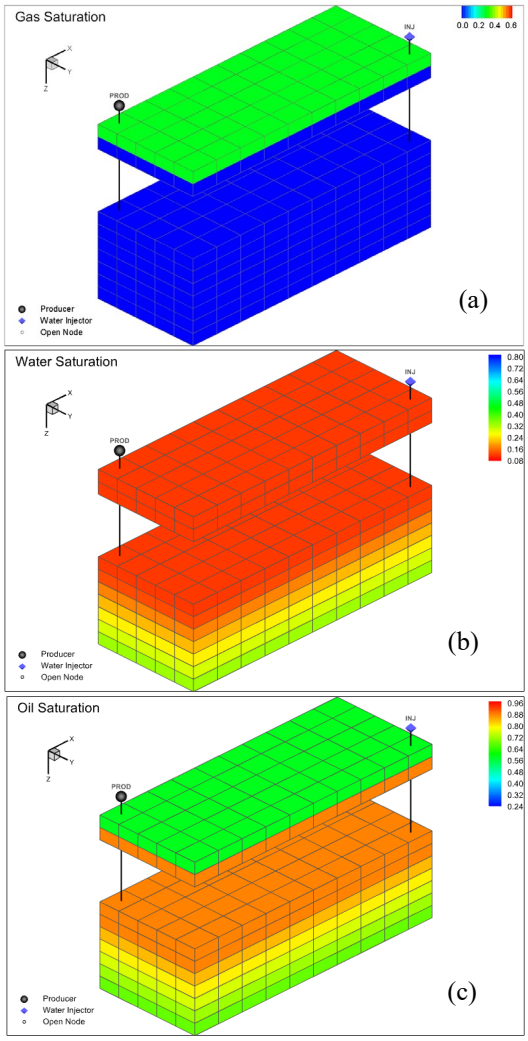

Fig. 9. Initial (a) water, (b) oil, and (c) gas saturation.

5. WELL MODEL IN OLGA

Figure 10 illustrates the pipe in the horizontal annulus. The annulus is the gap between the wellbore and the surface. Since OLGA does not have a method to simulate the flow through the annulus and inflow control devices, the OLGA model is developed to separate pipelines called wellbore and production tubing (Anuththara *et al.*, 2023).

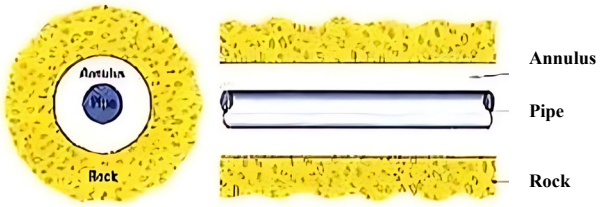

Fig. 10. Pipe in the horizontal annulus.

5.1 Compositional settings

The three black oil components (gas, oil, and water) are defined for the simulations. No gas has been injected into the reservoir; only oil and water feed rates are given. Compositions of the feeds are as in Table 3.

Table 3. Oil and water feed components.

Feed	Gas fraction	Water cut
Oil	50 Sm^3/ Sm^3 (GOR)	0.0001
Water	0.0001 Sm^3/Sm^3 (GLR)	0.99

5.3 Flow component settings

Since the three laterals are modelled and studied for oil production, each lateral consists of a wellbore and production tubing. The length and diameter of each wellbore are 625 m and 0.2159 m, respectively. The top and bottom production tubing are the same length as the wellbore, while the middle length is 500 m. The junction node connects the three laterals into one production pipe.

The description of each lateral is illustrated in Table 4 below.

Table 4: Technical description of the wellbore and production tubing

SN	Pipe name	Diameter (m)	Roughness (μm)	Elevation (m)
1	Wellbore top	0.2159	15	
	Production tubing	0.1397	15	10
2	Wellbore top	0.2159	15	
	Production tubing	0.1397	15	80
3	Wellbore top	0.2159	15	
	Production tubing	0.1397	15	110
4	Outlet production tubing	0.1397	15	10

The oil is assumed to be produced from 5 zones with one inflow control device. Two packers isolate the wellbore to stop the fluid from flowing to different zones. Near well source uses the data given by ECLIPSE to connect OLGA with ECLIPSE. Then, the fluid enters the wellbore after passing the inflow control device in the first section. The reservoir fluids enter the production tubing through a leak in the second section, as shown in Fig. 11.

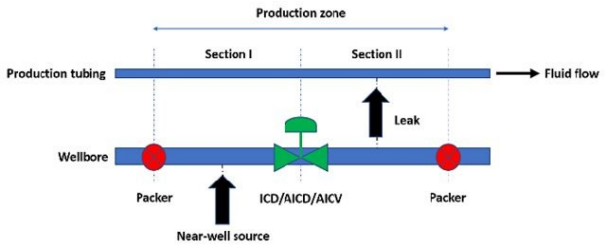

Fig. 11. Layout for one production zone.

6. RESULTS AND DISCUSSION

This chapter shows and discusses the results obtained from the OLGA-ECLIPSE model. The functionality of ICD, AICD, and AICV was discussed, and the results obtained for 500 days were compared. AICV showed better results within the given circumstances in this case, as expected.

6.1 Oil production

Figure 12 illustrates the oil production rates for the FCDs studied in this work for 500 days. Initially, oil production for all the FCDs showed similar rates because the water breakthrough had not yet occurred. However, the oil production rate decreased with the water breakthrough at around 160 - 180 days. As seen in Fig. 12, AICV shows a lower value for oil production, which is undesirable for AICV because AICV chokes the flow when it consists of low viscous fluids like water. However, the simulation was done for only 500 days, insufficiently covering the whole lifetime of the reservoir. However, AICV obtained a better oil fraction despite low oil production.

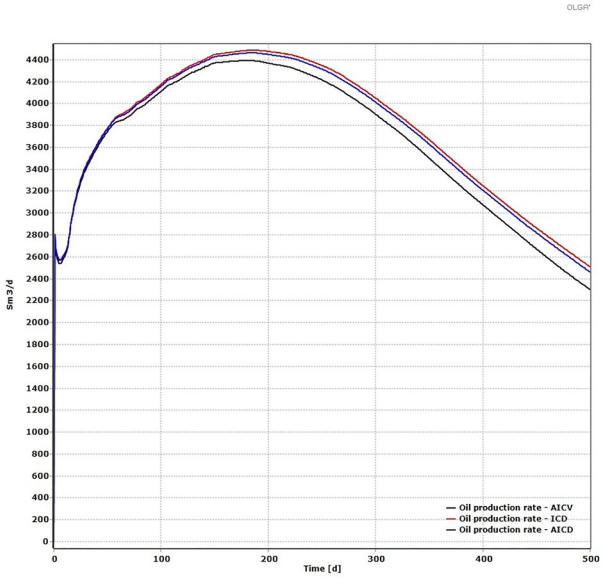

Fig. 12. Oil production rates for ICD, AICD, and AICV models.

Similarly, Figure 13 presents the accumulated oil production for each device over 500 days. AICV showed low oil production primarily due to its choking function when there is more water.

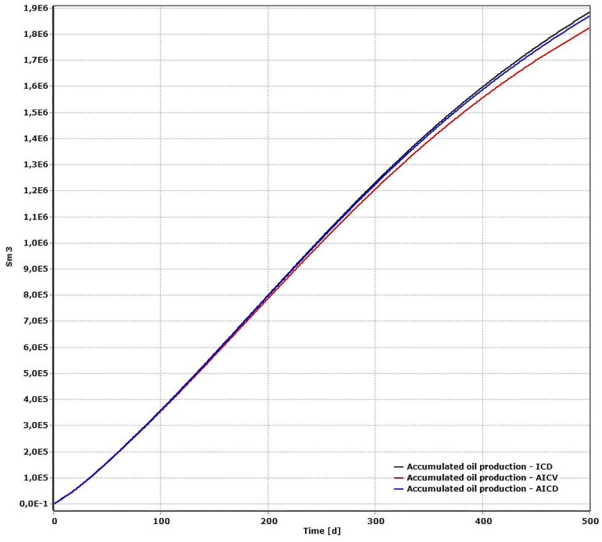

Fig. 13. Accumulated oil production over 500 days for ICD, AICD, and AICV.

6.2 Water production

The water production rates for 500 days for each control device are illustrated in Fig. 14. A small amount of water is produced even before the water breakthrough because of the water from the bottom lateral. However, the water production

increased significantly for each FCD with the water breakthrough. Nevertheless, after the water breaks through, the production rate increases significantly, and AICV showed a low water production rate increase compared to other FCDs.

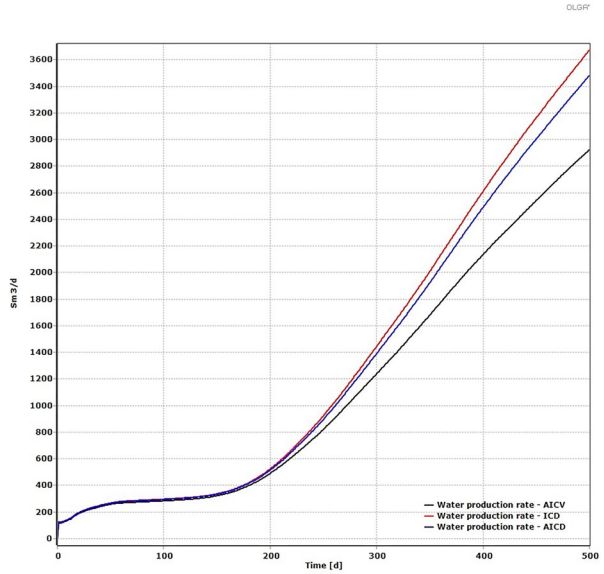

Fig. 14. Water production rates for 500 days for ICD, AICD, and AICV.

Figure 15 illustrates water accumulation over 500 days, and AICV showed lower water accumulation than AICD and ICD.

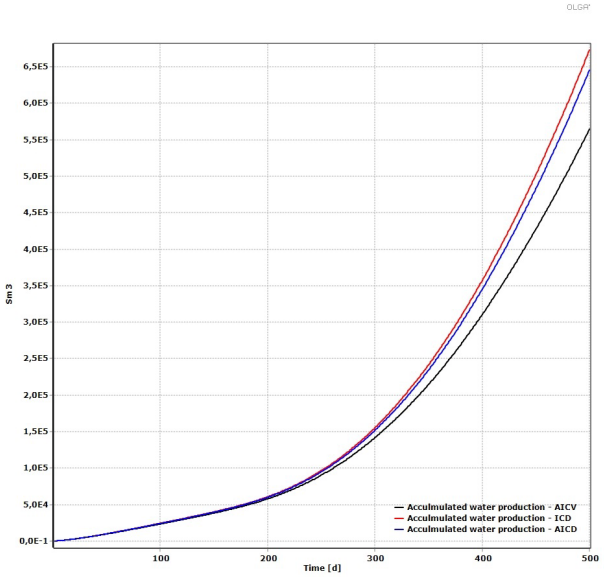

Fig. 15. Accumulated water production for ICD, AICD, and AICV for 500 days.

6.3 Total liquid production

With no liquid production cap defined, AICV showed the lowest liquid production, as shown in Fig. 16 and 17. Figure 16 represents the total liquid production rate, and Figure 17 shows the total accumulated liquid production. AICV shows low production because, after the water breakthrough, the water amount in the mixture is higher.

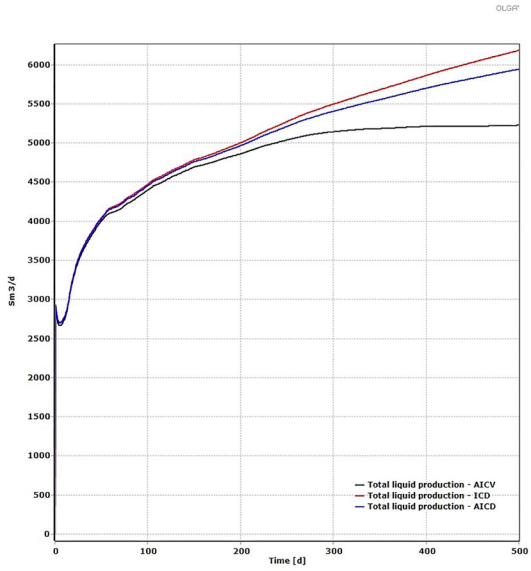

Fig. 16. Total liquid production rates for 500 days for ICD, AICD, and AICV.

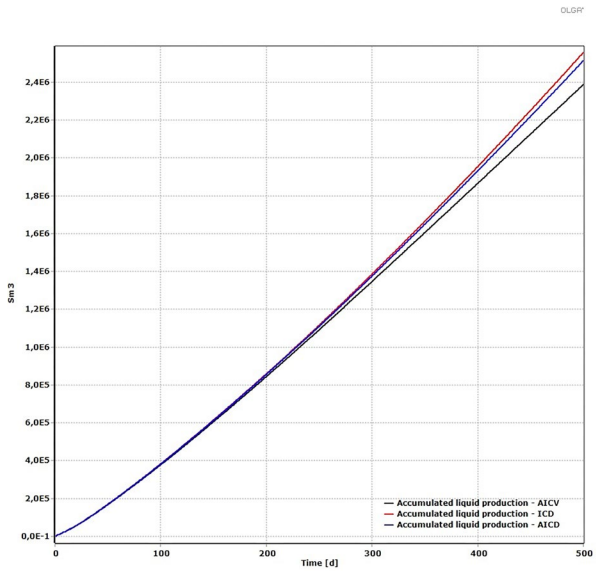

Fig. 17. Total accumulated liquid production for 500 days for ICD, AICV, and AICV.

6.4 Water cut variations

Keeping the water cut at its minimum is essential in the oil and gas industry as it impacts the overall economy and environmental sustainability. Figure 18 illustrates the water cut variation in the outlet for each FCD during 500 days of production. According to the Fig. 18, AICV, represented by solid colours, shows the lowest water cut along three laterals at almost every point compared with other FCDs. AICD represents continuous dotted lines showing the second lowest water cut along the tubes, while the well with ICD shows the highest water cut throughout all the production tubes because AICV has a higher choking ability with the water cut than AICD, while ICD does not have a choking ability.

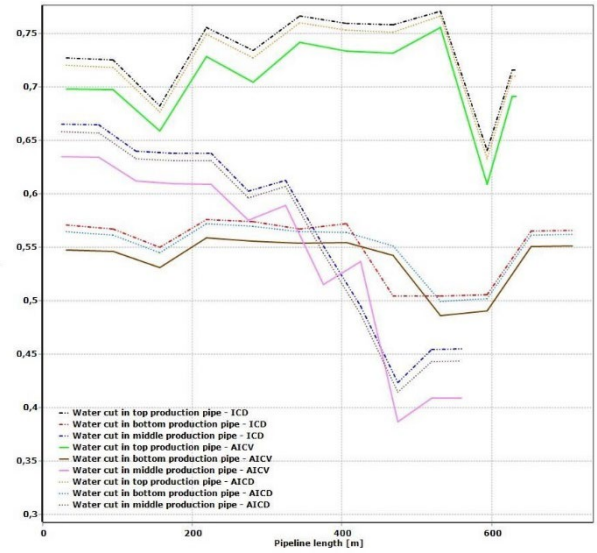

Fig. 18. Water cut (WC) variation along all the laterals for ICD, AICD, and AICV.

6.5 Fluid saturations

Figure 19 shows the oil saturation after 500 days in the reservoir simulated in ECLIPSE, while Fig. 20 shows the oil saturation along the horizontal plain of the three laterals. Compared to Fig. 9, the oil levels seem very low in the grid cells after 500 days of operation due to oil recovery.

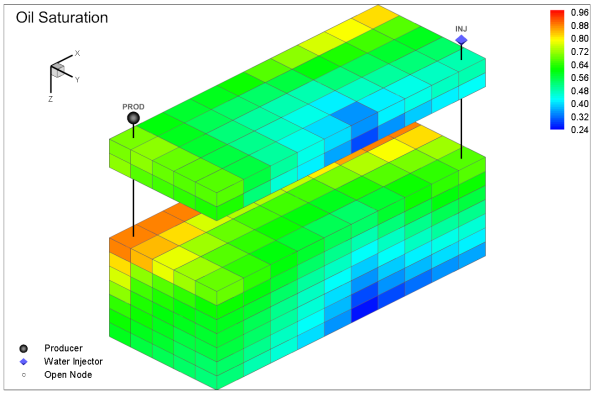

Fig. 19. Oil saturation in the reservoir after 500 days.

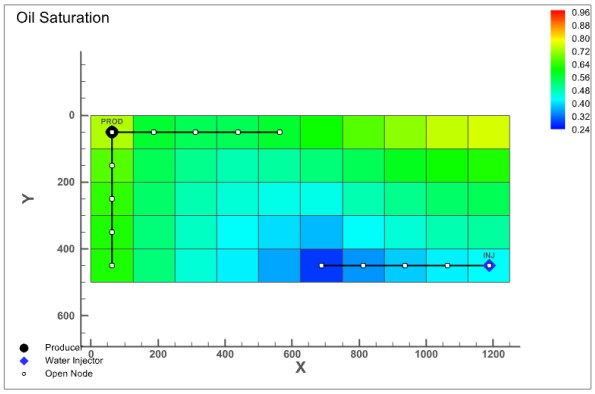

(a)

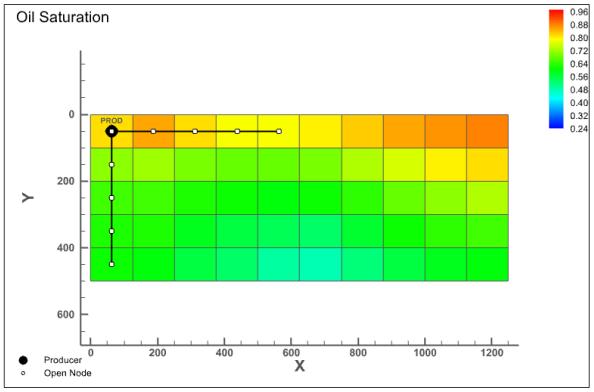

(b)

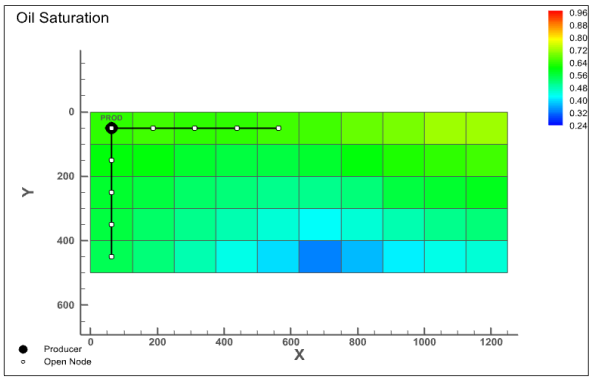

(c)

Fig. 20. Oil saturation in the horizontal layer around the (a) top, (b) middle, and (c) bottom laterals after 500 days.

Similarly, Figure 21 represents the water saturation after 500 days in the reservoir in three dimensions, while Fig. 22 shows the water saturation along the horizontal plain of the three laterals. Compared to Fig. 9, the water levels seem very high in the grid cells after 500 days of operation, mainly because of the water injection.

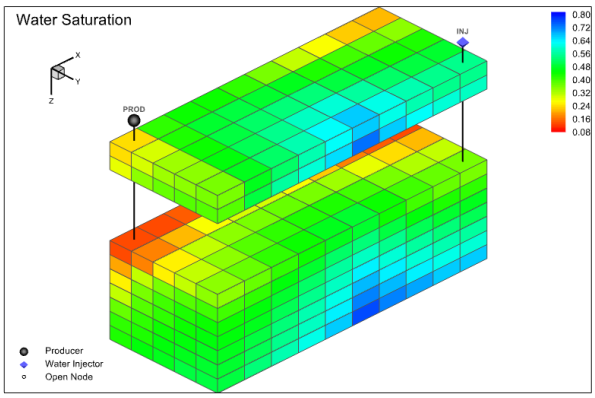

Fig. 21. Water saturation in the reservoir after 500 days.

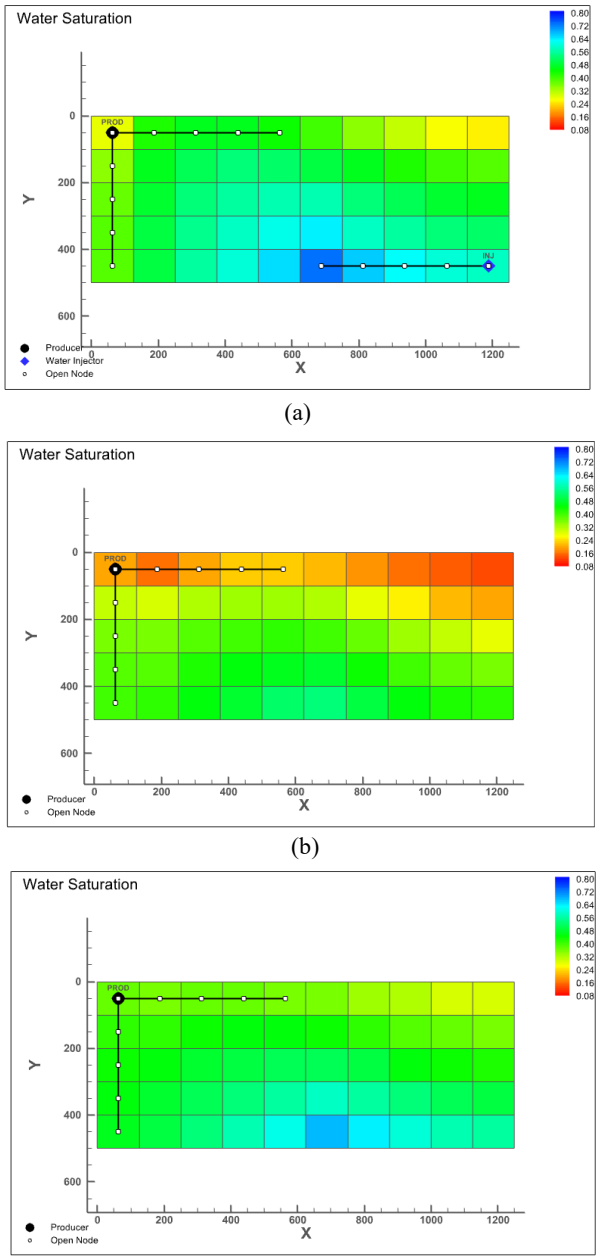

(a)

(b)

(c)

Fig. 22. Water saturation in the horizontal layer around the (a) top, (b) middle, and (c) bottom laterals after 500 days.

6.6 Chocking Effects of FCDs

Figure 23 shows how FCDs in similar locations at the top lateral (first and third FCD) for AICD and AICV perform with the water cut, and it shows that AICV has closed its opening up to 0.4 and AICD up to 0.12 for a water cut around 0.8 near third valve. Furthermore, near first valve, for a water cut around 0.67, AICD closed its opening up to 0.12 and AICV up to 0.35. As Fig. 5 mentions, AICV chokes its opening more than AICD does when more water is present. Therefore, the results obtained in Fig. 23 agree with the FCD functionalities.

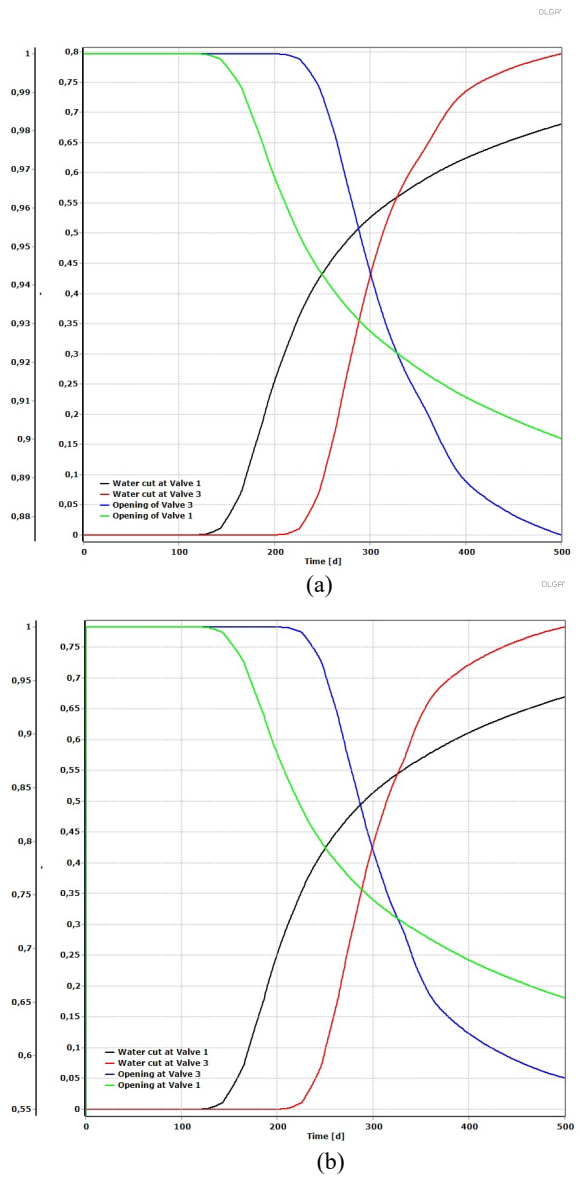

(a)

(b)

Fig. 23. Choking effect on (a) AICD and (b) AICV with the relevant water cuts.

7. CONCLUSIONS

Water breakthroughs are a significant challenge in the oil and gas industry, and various inflow control devices (ICDs, AICDs, and AICVs) are designed to mitigate this issue. ICDs balance drawdown pressure and fluid flow but cannot block water once it enters the well. AICDs and AICVs can choke water entry, reducing water production and delaying water breakthrough. AICVs are more effective than AICDs in choking low-viscosity fluids.

The study simulated a simple reservoir and multilateral well for 500 days, observing the effects of ICDs, AICDs, and AICVs on oil and water production rates and water cuts. Results showed that AICV had the lowest water cut (0.539) compared to AICD (0.566) and ICD (0.573) and the lowest production rates with 2302 m^3/day for oil and 2919 m^3/day for water. Although AICVs performed unexpectedly due to the

short simulation period, they are expected to perform better over a more extended period with production limitations.

The study concluded that AICVs are the most effective in reducing water production, making them economically and environmentally viable. It recommended simulating reservoirs for at least 2000-3000 days for better results and proposed further work on gas injection and actual case simulations to benefit the industry. The primary objective of coupling OLGA and ECLIPSE was to model an advanced multilateral well and simulate the reservoir, and the well was successfully achieved.

ACKNOWLEDGMENTS

We sincerely thank the Research Council of Norway and Equinor for their financial support through Research Council Project No. 308817, Digital Wells for Optimal Production and Drainage (DigiWell). We also appreciate the University of South-Eastern Norway for providing the essential software arrangements for this work.

REFERENCES

Elyasi, S. (2016). Assessment and evaluation of degree of multilateral well's performance for determination of their role in oil recovery at a fractured reservoir in Iran, *Egyptian Journal of Petroleum*, 25(1), pp. 1–14. doi: 10.1016/j.ejpe.2015.06.006.

Von Flatern, R., (2021). Defining Multilateral Wells [WWW Document]. URL https://www.slb.com/resource-library/oilfield-review/defining-series/defining-multilateral-wells (accessed 04.03.24).

Aakre, H., Halvorsen, B., Werswick, B., and Mathiesen, V. (2014). Autonomous Inflow Control Valve for Heavy and Extra-Heavy Oil, *SPE Heavy and Extra Heavy Oil Conference: Latin America*, OnePetro. doi: 10.2118/171141-MS.

Anuththara, M., Moradi, A., Kumara, A.S., and Moldestad, B.M.E. (2023). Simulation of Oil Recovery Through Advanced Wells Using a Transient Fully Coupled Well-Reservoir Model, *Scandinavian Simulation Society*, pp. 86–93. doi: 10.3384/ecp200012.

Moradi, A., Tavakolifaradonbe, J., and Moldestad, B.M.E. (2022a). Data-Driven Proxy Models for Improving Advanced Well Completion Design under Uncertainty, *Energies*, 15(20), p. 7484. doi: 10.3390/en15207484.

Mathiesen, V., Werswick, B., and Aakre, H. (2014). The Next Generation Inflow Control, the Next Step to Increase Oil Recovery on the Norwegian Continental Shelf, *SPE Bergen One Day Seminar*, OnePetro. doi: 10.2118/169233-MS.

Moradi, A., Samani, N.A., Kumara, A.S., and Moldestad, B.M.E. (2022b). Evaluating the performance of advanced wells in heavy oil reservoirs under uncertainty in permeability parameters, *Energy Reports*, 8, pp. 8605–8617. doi: 10.1016/j.egyr.2022.06.077.